文章编号：1001－9014(2017)02－0144－05

DOI:10.11972/j.issn.1001－9014.2017.02.004

Effect of cation ratio on structural and electrical properties of $Mn_x Co_y Ni_{3-x-y} O_4$ thin films

ZHANG Fei, WU Jing, OUYANG Cheng, ZHOU Wei, GAO Yan-Qing, HUANG Zhi-Ming*

(National Laboratory for Infrared Physics, Shanghai Institute of Technical Physics, Chinese Academy of Sciences, Shanghai 200083, China)

Abstract: Thin films of Mn-Co-Ni-O (MCNO) with different cation ratios were deposited by the magnetron sputtering method. By analyzing the material structure, it can be found that the grain size grows gradually with increasing Co cation number with constant Mn cation number, while the lattice parameter grows first and then decreases. The preferential orientation of thin films changes from (311) plane to (400) plane with increasing Mn cation number and the properties of thin films are unstable when the Co cation number is constant. The electrical properties show that both of Mn cations and Co cations participate in the conductivity, and $Mn_{1.2}Co_{1.5}Ni_{0.3}O_4$ has the lowest resistivity (235 Ω · cm) as well as the highest negative temperature coefficient of resistance (NTCR) $|\alpha_{295}|$ (4.7% · K^{-1}) at room temperature.

Key words: MCNO thin films, electrical properties, resistivity, activation energy

PACS: 61.80.Az

不同离子比的锰钴镍薄膜材料结构和电学性能

张 飞, 吴 敬, 欧阳程, 周 炜, 高艳卿, 黄志明*

(中国科学院上海技术物理研究所 红外物理国家重点实验室,上海 200083)

摘要:采用磁控溅射法分别制备了不同组分的Mn-Co-Ni-O(MCNO)薄膜材料.通过对材料结构分析,发现在Mn离子数目不变的情况下,随着Co离子的增加,晶粒尺寸逐渐增大,且晶格常数先增大后减小;在Co离子数目不变的情况下,随着Mn离子的增加,薄膜的择优生长晶面由(311)不晶面向(400)晶面转变.对电学性能测试进行分析,可知薄膜材料既有Mn离子的导电机制,也有Co离子的导电机制;$Mn_{1.2}Co_{1.5}Ni_{0.3}O_4$ 具有最低的电阻率(235 Ω·cm),具有最高的室温负温度电阻系数 $|\alpha_{295}|$ (4.7% · K^{-1})值.

关 键 词:MCNO薄膜;电学特性;电阻率;激活能

中图分类号:TN21 **文献标识码**:A

Introduction

Mn-Co-Ni-O (MCNO) materials belong to AB_2O_4 cubic spinel structure. They have excellent negative resistance temperature characteristic which is extensively used as uncooled infrared detector and surge protection devices[1-2]. Compared with bulk materials, MCNO thin films deposited by the magnetron sputtering method have fewer defects and more excellent electrical performance[3]. Lots of studies about MCNO thin films have been conducted and the polaron hopping theory has been extensively accepted—the hopping of electrons from Mn^{3+} to Mn^{4+} in octahedron is considered to be the reason of conductivity[4-6]. Most of the researches focused on the effect of Mn cation, but few studied about the effects of Co cation and Ni cation[6-7]. R. Schmid pointed out that the cation distribution in cubic $NiMn_2O_{4+\delta}$ spinel structure can affect the number of Mn^{3+}/Mn^{4+} cation pair[4]. R. D. Shannon pointed out that the chemical composition regulates the charge carrier number at high temperature[8]. However, the effects on conduction

Received date: 2016-06-08, **revised date**: 2016-12-13 **收稿日期**:2016-06-08, **修回日期**:2016-12-13

Foundation items: Supprted by Shanghai project(15ZR1445700), SITP Innovation seed fund, and National Natural Science foundation of China (61274138, 11304336)

Biography: ZHANG Fei(1986-), male, Henan, China, doctoral candidate. Research aren involves thermal Sensitive material and device.

* **Corresponding author**: E-mail: zmhuang@mail.sitp.ac.cn

of MCNO thin films for Mn, Co, and Ni cations are still unclear. In this paper, we invested the effect on structural and electrical properties of MCNO films by changing the number ratio of Mn, Co and Ni cations which will facilitate finding out the best number ratio for MCNO thin films with as low resistivity as possible and also will improve the properties of uncooled infrared detector made of MCNO thin films.

1 Experimental

$Mn_xCo_yNi_{3-x-y}O_4$ thin films were grown on substrate by sputtering deposition (LAB Line SPUTTER 5 magnetron, Kurt J. Lesker Company). The sputter target size was Φ100 mm. The substrate was amorphous Al_2O_3 slice with the thickness 200 μm and the dimension is 20 × 20 mm^2. High purity (>99.99%) argon gas was ventilated with 7 SCCM volume flow when the vacuum pressure was 9×10^{-8} Torr. The sputtering power was 50 W and the substrate temperature was room temperature with 5 r/min rotate speed to ensure the uniformity of sputtering thin films. The sputtering time of 10 hours was used to achieve a thickness (725 ± 20) nm. The final ion ratios of thin films are (x, y) = (2, 0.7), (1.5, 1), (1.2, 0.7), (1.2, 1.2), (1.2, 1.5), (1, 2), (0, 2), (2, 0).

The deposited MCNO thin films were annealed under 750℃ in air for 15 minutes, and then cooled to room temperature without control. XRD diffraction (XRD, D8 Advance) was conducted on annealed thin films and the surface morphology was observed by high resolution field emission scanning electron microscopy (SEM, FEI Sirion 200). The voltage-current curve of the samples was measured by a Keithley 2400 source meter at variable temperature controlled with a Lakeshore 330 system. The temperature range was from 180 K to 320 K.

2 Results and discussion

2.1 Structure

Figure 1 shows the XRD patterns of the MCNO films. It can be seen that the diffraction peaks are mainly corresponding to (311), (400), (222), (220), (511), (111), (440) lattice planes, which means that all these films are cubic spinel structure[9]. The (400) peak is the strongest for the films (x, y) = (1.5, 1) and (1, 2). The (311) peak is the strongest for the rest ones. It means that the preferential growth direction is (400) lattice plane for $Mn_{1.5}Co_1Ni_{0.5}O_4$ and $MnCo_2O_4$ thin films, while the preferential growth direction is (311) lattice plane for the rest samples. The preferential growth direction is related with the lowest surface energy. It means that the lowest surface energy for $Mn_{1.5}Co_1Ni_{0.5}O_4$ and $MnCo_2O_4$ thin films is (400) lattice plane while the lowest surface energy for the rest samples is (311) lattice plane. When x = 1.2 (Mn cation number is invariable), both of (111) peak and (222) peak decrease gradually with increasing Co cations (Co^{2+}/Co^{3+}), however, the (400) peak increases with growing Co cations. For (311) peak, the full width at half maximum (FWHM) decreases with growing Co cations. When y = 0.7, the FWHM is 0.4°; when y = 1.2, the FWHM is 0.32°; when y = 1.5, the FWHM is 0.18°. The grain size can be calculated to be 30 nm, 38 nm, 67 nm, respectively, which basically coincides with the grain size shown in Fig. 2. It illustrates that the grain size increases with growing Co cation number and invariable Mn cation number.

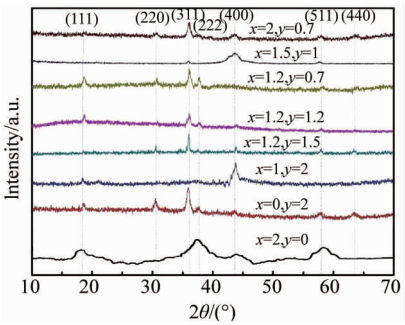

Fig. 1　XRD patterns of $Mn_xCo_yNi_{3-x-y}O_4$ thin films
图 1　$Mn_xCo_yNi_{3-x-y}O_4$ 薄膜材料的 XRD 衍射图

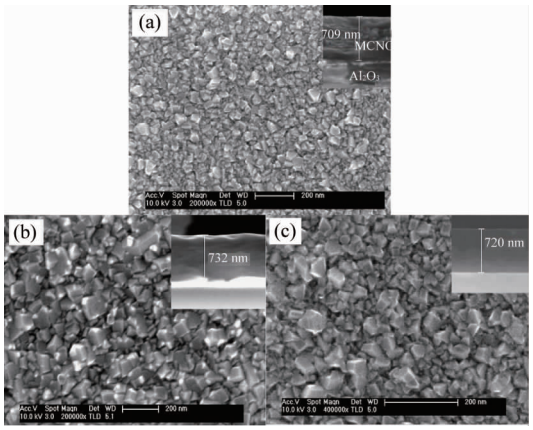

Fig. 2　SEM micrographs of (a) $Mn_{1.2}Co_{0.7}Ni_{1.1}O_4$, (b) $Mn_{1.2}Co_{1.2}Ni_{0.6}O_4$, (c) $Mn_{1.2}Co_{1.7}Ni_{0.3}O_4$. Inset: the numbers show the thicknesses of the MCNO film. The substrate is Al_2O_3 slice
图 2　SEM 图像 (a) $Mn_{1.2}Co_{0.7}Ni_{1.1}O_4$, (b) $Mn_{1.2}Co_{1.2}Ni_{0.6}O_4$, (c) $Mn_{1.2}Co_{1.7}Ni_{0.3}O_4$. 右上角插图标注为薄膜厚度,衬底为 Al_2O_3 片

The (311) peak of $MnCo_2O_4$ (x = 1, y = 2) thin films will weaken while the (400) peak will be strengthen compared with $NiCo_2O_4$ (x = 0, y = 2) thin films. It means that the preferential growth direction changes from (311) lattice planes to (400) lattice planes with growing Mn cation number and invariable Co cation number, and the trend also appears between $Mn_2Co_{0.7}Ni_{0.3}O_4$ (x = 2, y = 0.7) and $Mn_{1.2}Co_{0.7}Ni_{1.1}O_4$ (x = 1.2, y = 0.7) thin films (Fig. 1). It illustrates that the surface energy of (400) lattice planes decreases with more and more Mn cations, but it increases for (311) lattice planes conversely. According to Fig. 3, the binding energy of Mn 2p peak becomes small for $Mn_2Co_{0.7}Ni_{0.3}O_4$ thin film compared with $Mn_{1.2}Co_{0.7}Ni_{1.1}O_4$ thin film and there are more Mn^{2+} and Mn^{3+} cations (Table 1) for $Mn_2Co_{0.7}$

$Ni_{0.3}O_4$ thin film. However, the binding energy of Co 2*p* peak becomes bigger conversely and there are more Co^{3+} cations for $Mn_2Co_{0.7}Ni_{0.3}O_4$ thin film. It can be concluded that Mn^{2+} and Mn^{3+} cations mainly locate on the (400) lattice planes and the increasing of Mn^{2+} and Mn^{3+} numbers lowers the surface energy, while Co^{3+} cation mainly locate on the (311) lattice planes and the increasing of Co^{3+} number enlarges the surface energy.

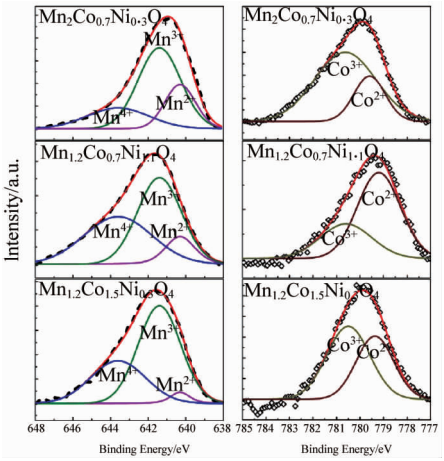

Fig. 3 XPS fitting of Mn $2p_{3/2}$ and Co$2p_{3/2}$ signals of $Mn_2Co_{0.7}Ni_{0.3}O_4$, $Mn_{1.2}Co_{0.7}Ni_{1.1}O_4$, $Mn_{1.2}Co_{1.5}Ni_{0.3}O_4$ thin films

图 3 $Mn_2Co_{0.7}Ni_{0.3}O_4$, $Mn_{1.2}Co_{0.7}Ni_{1.1}O_4$, $Mn_{1.2}Co_{1.5}Ni_{0.3}O_4$薄膜的 XPS 谱中 Mn $2p_{3/2}$和 Co$2p_{3/2}$峰拟合

Table 1 The proportion of Mn^{2+}、Mn^{3+}、Mn^{4+} cations as well as the proportion of Co^{2+}、Co^{3+} cations for $Mn_2Co_{0.7}Ni_{0.3}O_4$, $Mn_{1.2}Co_{0.7}Ni_{1.1}O_4$, $Mn_{1.2}Co_{1.5}Ni_{0.3}O_4$ thin films

表 1 $Mn_2Co_{0.7}Ni_{0.3}O_4$、$Mn_{1.2}Co_{0.7}Ni_{1.1}O_4$、$Mn_{1.2}Co_{1.5}Ni_{0.3}O_4$各薄膜中 Mn^{2+}、Mn^{3+}、Mn^{4+} 离子的比例关系及 Co^{2+}、Co^{3+}离子的比例关系

	Mn^{2+}	Mn^{3+}	Mn^{4+}	Co^{2+}	Co^{3+}
$Mn_2Co_{0.7}Ni_{0.3}O_4$	21%	57%	22%	25%	75%
$Mn_{1.2}Co_{0.7}Ni_{1.1}O_4$	10%	49%	41%	68%	32%
$Mn_{1.2}Co_{1.5}Ni_{0.3}O_4$	4%	62%	34%	43%	57%

2.2 Electrical properties

Figure 4 shows that the order of resistivity value for $NiMn_2O_4$, $MnCo_2O_4$, $NiCo_2O_4$ thin films is $\rho_{NiMn2O4} > \rho_{MnCo2O4} > \rho_{NiCo2O4}$. Jing Wu proposed that the electron hopping between Mn^{4+} and Mn^{3+} cations in octahedron is responsible for the conductive mechanism of $NiMn_2O_4$ thin film[10]. For $NiCo_2O_4$ thin film, the conductive mechanism is not very clear. Lin-Feng Hu thought that it is the excitation of electrons between the high-spin and low-spin states of Co^{3+} in octahedron which can be described by the nearest-neighbor hopping (NNH) model and variable-range hopping (VRH) model, and the NNH will become more prominent with increasing temperature[11]. The resistivity of $NiCo_2O_4$ thin film is the minimum among the three samples which means that the charge carrier produced by Co cations are more than those produced by Mn cations. This may results from the disparity of capability for Co and Mn cations to occupy the octahedron or from the interaction among cations. However, the resistivity of $MnCo_2O_4$ thin film lies in between due to the coexistence of Mn and Co cation conductive mechanisms.

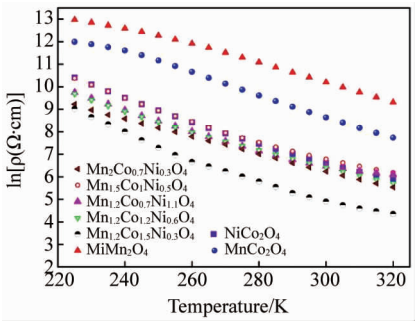

Fig. 4 Curves of ln(ρ) VS. Temperature

图 4 ln(ρ) VS. Temperature 图像

From Fig. 4, we can also get some points as follows. (1) When the Mn cation content is invariable ($Mn_{1.2}Co_{0.7}Ni_{1.1}O_4$, $Mn_{1.2}Co_{1.2}Ni_{0.6}O_4$, $Mn_{1.2}Co_{1.5}Ni_{0.3}O_4$, $x=1.2$), the MCNO film resistivity decreases with increasing Co cation content above 220 K. Firstly, it accounts for the augment of the number of Mn^{3+}, Mn^{4+} and Co^{3+} cations (Fig. 3 and Table 1) which result in the conduction of the MCNO film. Secondly, the increasing of Co cations can enlarge the grain size (Fig. 2) and it will reduce the specific surface area of the grain boundary and bring about a reduced electron scattering. (2) When the Co cation content is invariable ($Mn_2Co_{0.7}Ni_{0.3}O_4$, $Mn_{1.2}Co_{0.7}Ni_{1.1}O_4$, $y=0.7$), the resistivity of $Mn_2Co_{0.7}Ni_{0.3}O_4$ ($x=2$) thin film is always lower than that of $Mn_{1.2}Co_{0.7}Ni_{1.1}O_4$ ($x=1.2$) thin film. It mainly due to the increased Co^{3+} cations and Mn^{3+} cations (Fig. 3 and Table 1) which will produce more polarons[12]. (3) When the total content of Mn and Co cations is invariable, such as $Mn_2Co_{0.7}Ni_{0.3}O_4$ ($x+y=2.7$) and $Mn_{1.2}Co_{1.5}Ni_{0.3}O_4$ ($x+y=2.7$) thin films, the resistivity will be lower for MCNO thin film with higher Co content. The total content of Mn and Co cations for $Mn_{1.5}Co_1Ni_{0.5}O_4$ ($x+y=2.5$) and $Mn_{1.2}Co_{1.2}Ni_{0.6}O_4$ ($x+y=2.4$) thin films can be considered as approximately equal with each other. It shows that the $Mn_{1.2}Co_{1.2}Ni_{0.6}O_4$ thin film has a low resistivity. The same rule is appropriate for $NiCo_2O_4$ ($x+y=2$) and $NiMn_2O_4$ ($x+y=2$) thin films, whose total content of Mn and Co cations are equal with each other. In Table 1, even though the ratio of Co^{3+} cation becomes small, it can be calculated that the total Co^{3+} cation number enlarges. Also both of Mn^{3+} and Mn^{4+} cation ratios increase. So the resistivity will be lower for MCNO thin film with high Co content when the total content of Mn and Co cations is invariable.

The negative temperature coefficient of resistance

(TCR) of MCNO thin films can be expressed as:

$$\alpha = \mathrm{d}R/R\mathrm{d}T \quad , \quad (1)$$

with 295 K as room temperature. Figure 5 is deduced from Fig. 4 at 295 K. It shows the changes of resistivity and TCR at room temperature (ρ_{295} and $|\alpha_{295}|$) for film samples. From Fig. 5, it can be seen that at small resistivity range (< 1000 Ω · cm), the $Mn_{1.2}Co_{1.5}Ni_{0.3}O_4$ thin film has the lowest resistivity (235 Ω · cm) and the highest $|\alpha_{295}|$ value (4.7% · K^{-1}). Although the $Mn_2Co_{0.7}Ni_{0.3}O_4$ thin film has low resistivity (400 Ω · cm), the $|\alpha_{295}|$ value (2.6% · K^{-1}) is still low. It also shows in Fig. 5 that when Mn cation number is invariable ($x = 1.2$), the change trends of resistivity and TCR are opposite with decreased Co cation number. When the total content of Mn and Co cations is almost invariable ($Mn_2Co_{0.7}Ni_{0.3}O_4$ and $Mn_{1.2}Co_{1.5}Ni_{0.3}O_4$, $Mn_{1.2}Co_{1.2}Ni_{0.7}O_4$ and $Mn_{1.5}Co_1Ni_{0.5}O_4$, $Mn_{1.2}Co_{0.7}Ni_{1.1}O_4$ and $NiCo_2O_4$), the $|\alpha_{295}|$ value is reduced with decreased Co cation number.

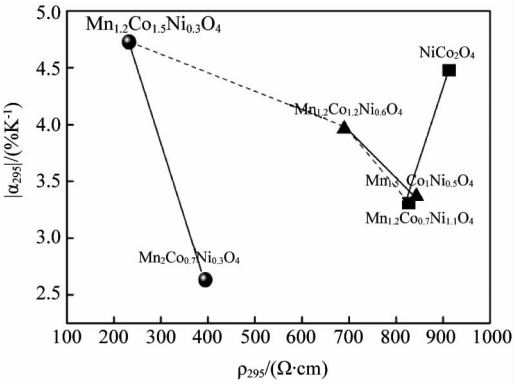

Fig. 5　Graphic of $|\alpha_{295}|$ VS ρ_{295}

图 5　$|\alpha_{295}|$ VS ρ_{295} 图

The polaron hopping conductions for Mn and Co cations can be described by NNH model and VRH model, and their expressions can be deduced as below[13]:

$$\rho(T) = CT^{\alpha}\exp(T_0/T)^p \quad , \quad (2)$$

where C is a constant and T_0 is a characteristic temperature of the thin film. For $a = p = 1$, it is the NNH model, and $\ln(\rho/T)$ has a linear relation with $1/T$. For $a = 2p$, it is the VRH model. According to the shapes of local density of states (LDOS), the VRH model can be separated into two models: uniform distribution for LDOS near Fermi level ($p = 0.25$) and parabolic distribution for LDOS near Fermi level ($p = 0.5$)[14]. There are linear relations for $\ln(\rho/T)$ vs $1/T$, $\ln(\rho/T)$ vs $1/T^{0.5}$ and $\ln(\rho/T)$ vs $1/T^{0.25}$ separately for corresponding conduction model and the T_0 value can be calculated as shown in Fig. 6. The T_c in Fig. 6 is the cut-off point for the NNH model and the VRH model, and is also the cut-off point for different activation energies. The T_c values are largely in 200 ~ 220 K except for $NiMn_2O_4$ (245 K) and $MnCo_2O_4$ (235 K). The T_0 values are different on both sides of T_c.

Figure 6 shows that, for $Mn_{1.2}Co_{0.7}Ni_{1.1}O_4$, $Mn_{1.2}Co_{1.2}Ni_{0.6}O_4$ and $Mn_{1.2}Co_{1.5}Ni_{0.3}O_4$ thin films whose Mn cations are invariable, the T_0 value will augment gradually with increasing Co cations in either NNH model or VRH model. It can be concluded that the conductivity activation energy of Co cation is larger than that of Mn cation for MCNO thin films. This is further confirmed by the fact that the T_0 value of $NiCo_2O_4$ thin film is higher than that of $NiMn_2O_4$ thin film.

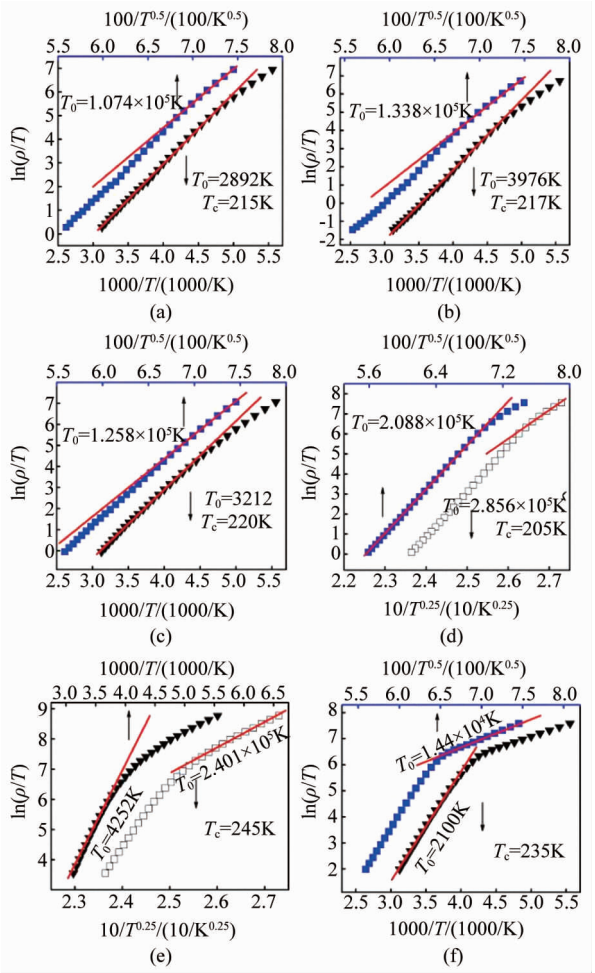

Fig. 6　T_c and T_0 values of $_Mn_xCo_yNi_{3-x-y}O_4$ thin films. (a) $Mn_{1.2}Co_{0.7}Ni_{1.1}O_4$, (b) $Mn_{1.2}Co_{1.2}Ni_{0.6}O_4$, (c) $Mn_{1.2}Co_{1.5}Ni_{0.3}O_4$, (d) $NiCo_2O_4$, (e) $NiMn_2O_4$, (f) $MnCo_2O_4$ (The solid triangles correspond to $p = 1$. The solid squares correspond to $p = 0.5$, The empty squares correspond to $p = 0.25$)

图 6　$Mn_xCo_yNi_{3-x-y}O_4$ 薄膜的 T_c 和 T_0 值 (a) $Mn_{1.2}Co_{0.7}Ni_{1.1}O_4$, (b) $Mn_{1.2}Co_{1.2}Ni_{0.6}O_4$, (c) $Mn_{1.2}Co_{1.5}Ni_{0.3}O_4$, (d) $NiCo_2O_4$, (e) $NiMn_2O_4$, (f) $MnCo_2O_4$ (实心三角对应 $p = 1$, 实心方形对应 $p = 0.5$, 虚方形对应 $p = 0.25$)

3　Conclusion

In summary, we prepared MCNO thin films with different cation ratios by the magnetron sputtering method and studied the structural and electrical properties. It can be found that the grain size increases first, and then decreases with growing Co cation number and invariable Mn cation number. The study of electrical properties

shows that both of Mn cation and Co cation contribute to MCNO thin film conductivity, and the charge carriers produced by Co cations are more than those produced by Mn cations. The conductivity activation energy of Co cation is larger than that of Mn cation for MCNO thin films.

References

[1] He L, Ling Z Y. Studies of temperature dependent ac impedance of a negative temperature coefficient Mn-Co-Ni-O thin film thermistor[J]. *Appl. Phys. Lett.*, 2011, **98**: 242112.

[2] Park K, Lee J K. The effect of ZnO content and sintering temperature on the electrical properties of Cu-containing $Mn_{1.95-x}Ni_{0.45}Co_{0.15}Cu_{0.45}Zn_xO_4$ ($0 \leqslant x \leqslant 0.3$) NTC thermistors[J]. *J. Alloys Compd.*, 2009, **475**: 513 - 517.

[3] Zhang F, Zhou W,. Annealing effect on the structural and electrical performance of Mn-Co-Ni-O films [J]. *AIP Advances*, 2015, **5**: 117137.

[4] Schmidt R, Basu A, Brinkman A W. Small polaron hopping in spinel manganates[J]. *Phys Rev B*, 2005, **72**(11):115101.

[5] Kong W W, Bu H J, Gao B, *et al*. Effects of preferred orientation on electrical properties of $Mn_{1.56}Co_{0.96}Ni_{0.48}O_4 \pm \delta$ spinel films[J]. *Materials Letters*, 2014, **137**: 36 - 40.

[6] Dannenberg R, Baliga S. Resistivity, thermopower and the correlation to infrared active vibrations of $Mn_{1.56}Co_{0.96}Ni_{0.48}O_4$ spinel films sputtered in an oxygen partial pressure series[J]. *J. Appl. Phys.*, 1999, **86**(1): 514 - 523.

[7] Zhou W, Xu X F, Yang C Q, *et al*. Annealing effect on the structural, electrical and 1/f noise properties of Mn - Co - Ni - O thin films[J]. *J Mater Sci: Mater Electron*, 2014, **25**(4): 1959 - 1964.

[8] Shannon R D. ucoz. ru Revised effective ionic radii and systematic studies of interatomic distances in halides and chalcogenides[J]. *Acta Crystallogr A*, 1976, **32**: 751 - 767.

[9] Chen L, Kong W W, Yao J C, *et al*. Synthesis and characterization of Mn-Co-Ni-O ceramic nanoparticles by reverse micro emulsion method [J]. Ceramics International, 2015, **41**: 2847 - 2851.

[10] Wu J, Huang Z M. Structural, electrical, and magnetic properties of $Mn_{2.52-x}Co_xNi_{0.48}O_4$ films [J]. *J. Appl. Phys.*, 2010, **107**(5): 053716-1-053716-6.

[11] Hu L F, Wu L M, Liao M Y, *et al*. Electrical transport properties of large, individual $NiCo_2O_4$ nanoplates [J]. *Adv. Funct. Mater.*, 2012, **22**(5):998 - 1004.

[12] Chen L, Kong W W, Yao J C, *et al*. Effect of sintering temperature on microstructure and electrical properties of $Mn_{1.2}Co_{1.5}Ni_{0.3}O_4$ ceramic materials using nanoparticles by reverse microemulsion method[J]. *J Mater Sci: Mater Electron*, 2016, **27**(2):1713 - 1718.

[13] Schmidt R, Basu A, Beinkman A W, *et al*. Electron-hopping modes in $NiMn_2O_{4+\delta}$ materials[J]. *Appl Phys Lett*, 2005, **86**(7):073501.

[14] Efros A L, Shklovskii B I. Coulomb gap and low temperature conductivity of disordered systems [J]. *J. Phys. C: Solid State Phys.*, 1975, **8**(4): L49 - L51.